

Ab initio nuclear shape coexistence and emergence of island of inversion around $N = 20$

E. F. Zhou,¹ C. R. Ding,¹ J. M. Yao,^{1,2,*} B. Bally,³ H. Hergert,^{2,4,†} C. F. Jiao,¹ and T. R. Rodríguez⁵

¹*School of Physics and Astronomy, Sun Yat-sen University, Zhuhai 519082, P.R. China*

²*Facility for Rare Isotope Beams, Michigan State University, East Lansing, Michigan 48824-1321, USA.*

³*ESNT, IRFU, CEA, Université Paris-Saclay, 91191 Gif-sur-Yvette, France.*

⁴*Department of Physics & Astronomy, Michigan State University, East Lansing, Michigan 48824-1321, USA.*

⁵*Departamento de Estructura de la Materia, Física Térmica y Electrónica,*

Universidad Complutense de Madrid, E-28040 Madrid, Spain.

(Dated: October 31, 2024)

We extend a nuclear *ab initio* framework based on chiral two- and three-nucleon interactions to investigate shape coexistence and the degradation of the $N = 20$ magic number in both even-even and odd-even neutron-rich nuclei. The quantum-number projected generator coordinate method, combined with the in-medium similarity renormalization group (IMSRG), is employed to compute their low-lying states. This approach successfully reproduces the coexistence of weakly and strongly deformed states at comparable energies, providing a natural explanation for the emergence of the $N = 20$ island of inversion through the IMSRG evolution of the chiral Hamiltonian. The results highlight the essential roles of both dynamic and static collective correlations in reproducing the ordering of nuclear states with distinct shapes. This work represents a significant advance in the application of *ab initio* methods to the intricate phenomenon of shape coexistence in medium-mass nuclei.

Introduction. The shapes of atomic nuclei are determined by the interplay between shell structure and collective correlations. In nuclei near closed shells, this interplay can give rise to the coexistence of different equilibrium shapes at similar energies, a phenomenon known as shape coexistence, which appears to be unique to finite quantum many-body systems [1]. A well-known example occurs in nuclei with neutron numbers around $N = 20$ magic number. For instance, ^{30}Mg [2] and ^{34}Si [3] exhibit near-spherical ground states that coexist with low-lying strongly deformed states arising from intruder configurations. In neutron-richer nuclei, such as ^{30}Ne [4], ^{31}Na [5], and ^{32}Mg [6], the ground states are dominated by intruder configurations involving two-particle-two-hole ($2p$ - $2h$) excitations across the $N = 20$ shell gap, indicating a degradation of the $N = 20$ magic number. These so-called “island-of-inversion” nuclei [7] have garnered significant attention over the past decades [8, 9]. In contrast to even-even nuclei, odd-mass nuclei in this region exhibit more complex low-energy structures, which remain poorly understood. This complexity is particularly evident in ^{33}Mg , where the spin-parity of the ground state has been a long-standing subject of debate [10–19], let alone the structure of its excited states. More generally, the low-energy structure of neutron-rich nuclei around $N = 20$ poses a formidable challenge for nuclear theories [9, 20–22].

In the past decade, significant progress has been made in the development of nuclear *ab initio* methods [23–30], which rely on nuclear interactions derived from chiral effective field theory [31–33]. One of the major remaining challenges for *ab initio* approaches is the accurate description of nuclear shape coexistence. Recently, the *ab initio* no-core shell model has been successfully applied to describe deformed rotational band in ^{20}Ne [34], as well as the coexistence of both normal and intruder states in ^{12}Be [35]. Nevertheless, extending this approach to heavier nuclei remains challenging due to the exponential growth in computational complexity with increasing

nucleon number A .

The in-medium similarity renormalization group (IMSRG) method [30, 36], which employs a flow equation to systematically decouple high-energy from low-energy degrees of freedom, has emerged as a promising *ab initio* approach for addressing heavier nuclei. In particular, the valence-space IMSRG (VS-IMSRG)[37–39] has been developed in conjunction with shell model to study open-shell nuclei, spanning a wide range of isotopes from the light to the heavy mass regions [40–42]. However, despite significant advancements, the VS-IMSRG, restricted to the normal-ordered two-body approximation (NO2B), encounters challenges in accurately describing the low-energy structure of strongly deformed nuclei [43–46]. This limitation can be overcome by using the multi-reference IMSRG (MR-IMSRG) [47], which was extended to deformed nuclei through its combination with the no-core shell model [48] and the quantum-number projected generator coordinate method (PGCM) [49, 50]. Other recently developed frameworks that seek to describe doubly open-shell nuclei through the simultaneous inclusion of both particle-hole excitation configurations and collective correlations are a novel many-body perturbation theory based on the PGCM [51–53], as well as the angular-momentum projected coupled cluster theory with singles and doubles (CCSD), which has been successfully applied to deformed even-even nuclei [54–56] and odd-mass nuclei [57]. While projected CCSD reproduces the low-energy structures of deformed nuclei, challenges remain in accurately describing shape coexistence, particularly in predicting the correct ordering for the energy levels associated with different shapes [57]. Furthermore, capturing the shape-mixing effect – essential for describing nuclear low-lying states with shape coexistence [58] – continues to pose a challenge for current implementations of these *ab initio* methods due to the complexity of the correlated wave function ansätze.

In this work, we extend the *ab initio* in-medium genera-

tor coordinate method (IM-GCM), which combines the MR-IMSRG and PGCM into a single consistent framework, to study shape coexistence in even-even and odd-even neutron-rich nuclei near neutron number $N = 20$. This method exploits the IMSRG to capture dynamic correlations associated with high-energy multi-particle multi-hole excitations and PGCM to include the collective (or static) correlations associated with pairing and deformation. The effectiveness of this approach is demonstrated through its application to the coexistence of near-spherical and strongly deformed states at similar energies. Notably, we find that the deformed ground state emerges naturally in the island-of-inversion nuclei with the IMSRG flow. Our study highlights the importance of both dynamic and collective correlations in accurately reproducing the low-lying states of nuclei with distinct shapes.

Methods. We start from an intrinsic nuclear many-body Hamiltonian that includes both two-body (NN) and three-body ($3N$) interactions. The NN interaction is based on the chiral $N^3\text{LO}$ potential by Entem and Machleidt [59], referred to as ‘EM’. We apply the free-space SRG [60] to evolve the EM interaction to a resolution scale of $\lambda = 1.8 \text{ fm}^{-1}$. The $3N$ interaction is constructed with a cutoff of $\Lambda = 2.0 \text{ fm}^{-1}$. The resulting Hamiltonian is labeled EM1.8/2.0 [61]. We normalize the $3N$ interaction with respect to a pre-selected reference state, retaining only the zero-, one-, and two-body terms. We explored two types of reference state: (i) an ensemble of multiple symmetry-restored Hartree-Fock-Bogoliubov states, determined through variation after particle-number projection (VAPNP) and subsequently projected also onto good angular momentum, and (ii) the ground state from a PGCM calculation. These are referred to as the ENO and GNO schemes, respectively. Our findings indicate that the ENO scheme outperforms the GNO scheme for nuclei exhibiting shape coexistence [62], and is thus employed in the remainder of the present analysis.

Using the normal-ordered Hamiltonian $H(0)$, we solve the IMSRG flow equation

$$\frac{dH(s)}{ds} = [\eta(s), H(s)], \quad (1)$$

via the Magnus expansion [49, 63]. The effective Hamiltonian evolved up to the flow parameter s is given by $H(s) \equiv U(s)H(0)U^\dagger(s)$, where the unitary transformation is assumed to be expressible as an explicit exponential of the Magnus operator $\Omega(s)$, $U(s) \equiv e^{\Omega(s)}$, instead of the general path-ordered exponential. The generator $\eta(s)$ is chosen to bring the reference states increasingly closer to the ground state as s increases. We employ the Brillouin generator, which ensures steepest descent in the energy $\langle H(s) \rangle$ of the (pure or mixed) ground state [64]. To keep the flow equation manageable, we truncate all operators at the NO2B level. For odd-mass nuclei, reference states are taken from neighboring even-even nuclei, a choice found to have minimal impact on the low-lying spectra of odd-mass nuclei. For further details, see Ref. [65] and the supplementary material [62].

Low-lying nuclear states are obtained through a subsequent

PGCM calculation based on the evolved Hamiltonian $H(s)$, where the wave functions are constructed as linear superpositions of the form

$$|\Psi_\alpha^{NZJM\pi}\rangle = \sum_c f_{\alpha c}^{NZJM\pi} \hat{P}_{MK}^J \hat{P}^N \hat{P}^Z |\Phi_\kappa(\mathbf{q})\rangle. \quad (2)$$

Here, α distinguishes states with same quantum numbers, and the symbol c is a collective label $c = \{K, \kappa, \mathbf{q}\}$ for different configurations, where \mathbf{q} represents the shape parameters. The mean-field wave functions $|\Phi_\kappa(\mathbf{q})\rangle$ are obtained from axial VAPNP calculations with conserved quantum numbers $\kappa = \Omega^\pi$ with Ω being the angular-momentum projection along z -axis and π the parity. The operators \hat{P}_{MK}^J and $\hat{P}^{N,Z}$ are projection operators that select components with angular momentum J and its third component M or $K = \Omega$, neutron number N and proton number Z [66, 67]. For odd-mass nuclei, the $|\Phi_\kappa(\mathbf{q})\rangle$ are one-quasiparticle states which can be obtained by exchanging one column of the U and V matrices starting from a Bogoliubov even-even vacuum [65, 66]. The weight functions $f_{\alpha c}^{NZJM\pi}$ are determined by varying the ground-state energy for the ansatz (2), which leads to the so-called Hill-Wheeler-Griffin equation [66, 68]

$$\sum_c \left[\mathcal{H}_{cc'}^{NZJ\pi} - E_\alpha^J \mathcal{N}_{cc'}^{NZJ\pi} \right] f_{\alpha c'}^{NZJM\pi} = 0, \quad (3)$$

where the expressions for the Hamiltonian and norm kernels can be found in Refs. [49, 65]. With the weight functions $f_{\alpha c}^{NZJM\pi}$ at hand, one can compute the electromagnetic moments and transition probabilities using appropriate evolved operators [43]. See Refs. [49, 50] and supplementary material [62] for more details.

Results and discussion. Nuclear low-lying states are highly sensitive to the underlying single-particle shell structure, which evolves with both the resolution scale of the chiral interaction and the flow parameter s in the IMSRG [69, 70]. Using the low-resolution chiral interaction EM1.8/2.0, we perform IM-GCM calculations for the low-lying states of ^{32}Mg . The ground state shows reasonable convergence as s increases, stabilizing around 0.16 MeV^{-1} [62]. Figures 1(a) and (b) display the energy curves and low-lying states for the two effective Hamiltonians $H(s)$ with $s = 0$ and 0.16 MeV^{-1} , respectively. Starting with the unevolved Hamiltonian $H(0)$, one observes in Fig. 1(a) that a weakly deformed ground state with an average axial deformation $\beta_2 \simeq 0.15$ (as defined in Ref. [71]) coexists with a strongly prolate-deformed excited 0^+ state with $\beta_2 \simeq 0.40$. As s increases to around 0.16 MeV^{-1} , the strongly prolate-deformed 0^+ state becomes the ground state. This inversion in the energy ordering between the two states can be attributed to changes in the single-particle shell structure, as shown in the Nilsson diagrams in Figs. 1(c) and (d). For the Hamiltonian evolved with $s = 0.16 \text{ MeV}^{-1}$, we can see a more pronounced downward slope of the $\Omega^\pi = 1/2^-$ component of the $\nu f_{7/2}$ orbital and a larger splitting between the $\Omega^\pi = 1/2^+$ and $3/2^+$ component of the $\nu d_{3/2}$ orbital with increasing β_2 . Consequently, a prolate deformed $N = 20$ shell gap opens up

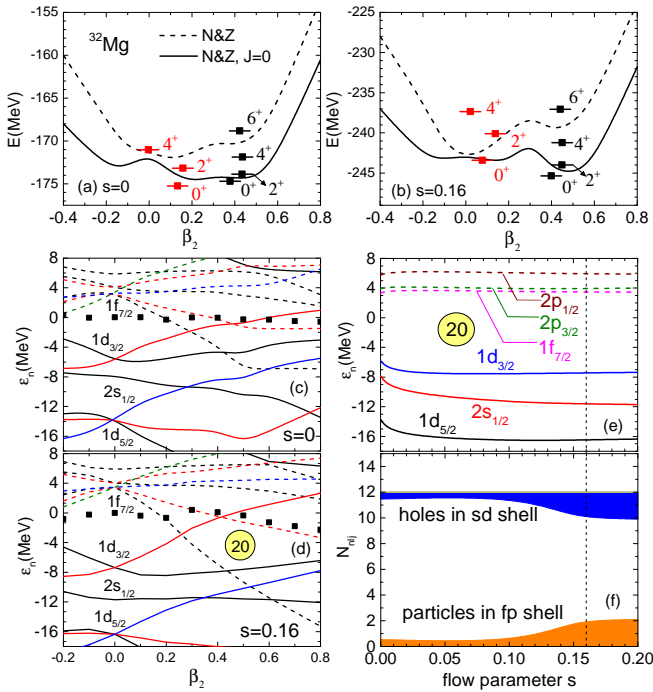


FIG. 1. Panel (a): Total energy as a function of the axial quadrupole deformation β_2 for the pure particle-number projected calculations (dashed) and those with additional projection onto $J = 0$ (solid) using the effective Hamiltonians $H(s)$ with IMSRG flow parameters $s = 0 \text{ MeV}^{-1}$. The low-lying states from the PGCM calculations are plotted at their mean quadrupole deformation $\bar{\beta}_2$. Panel (b): Same as (a), but for $s = 0.16 \text{ MeV}^{-1}$. Panel (c): Neutron Nilsson diagram for the $s = 0 \text{ MeV}^{-1}$ calculations. The Fermi energies are indicated with black squares. Panel (d): Same as (c), but for $s = 0.16 \text{ MeV}^{-1}$. Panel (e): Evolution of single-particle energy states for $\beta_2 = 0$ as a function of s . Panel (f): Evolution of neutron holes (blue area) in the sd shell and particles (orange area) in the fp shell in the IM-GCM ground state as a function of s . See the main text for details.

around $\beta_2 \approx 0.5$, which drives the development of a strongly prolate-deformed ground state.

We also present the evolution of single-particle energies for the spherical state in Fig. 1(e), in which an increased spin-orbit splitting is shown. It is important to note that, because our IM-GCM framework captures collective correlations by incorporating deformed configurations, the single-particle energies for spherical configurations provided here cannot be directly compared to the so-called effective single-particle energies in the valence-space shell model [73]. Instead, we offer an alternative, intuitive comparison with the shell model. As shown in Fig. 1(f), the number of holes in the sd shell, and the number of particles in the fp shell, as determined by diagonalizing the one-body density of the ground state, increases to around two with $s = 0.16 \text{ MeV}^{-1}$. From the shell-model perspective, changes in occupancy would influence the monopole interaction, leading to an evolution of effective single-particle energies and a reduction in the $N = 20$ shell gap [7, 8, 73]. Our calculations indicate that the ground state of ^{32}Mg is predominantly characterized by a $2p\text{-}2h$ excitation across the

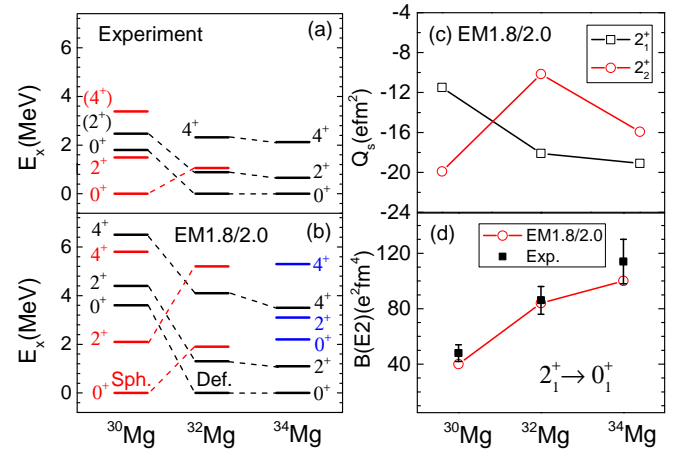


FIG. 2. Panel (a): Experimental low-lying energy spectra of $^{30,32,34}\text{Mg}$. Panel (b): Same as (a), but for the IM-GCM calculation. The states dominated by the configurations of near-spherical, moderately and strongly prolate shapes are indicated with red, blue and black colors, respectively. Panel (c): Calculated quadrupole moments Q_s for the 2_1^+ and 2_2^+ states. Panel (d): Reduced transition probability $B(E2 : 2_1^+ \rightarrow 0_1^+)$. Experimental data are taken from Ref. [72].

$N = 20$ shell gap, aligning with the traditional shell-model interpretation.

We extend the above study to the low-lying states of $^{30,34}\text{Mg}$, which are displayed in Fig. 2. Notably, the onset of large deformation from ^{30}Mg to ^{34}Mg is indicated by the increase in $B(E2 : 2_1^+ \rightarrow 0_1^+)$, and the absolute value $|Q_s(2_1^+)|$ of the spectroscopic quadrupole moment of the 2_1^+ state, as well as by the decrease in excitation energy $E_x(2_1^+)$, though the latter is systematically overestimated by 50%. This finding aligns with previous studies of ^{48}Ti [50] and ^{76}Ge [74], where it was shown that configuration mixing with a nonzero cranking frequency can compress excitation energies by a factor of 1.3 – 1.6, as discussed in more detail in the supplementary material [62]. Recent VS-IMSRG studies [75, 76] indicate that the excitation energy of 2_1^+ state can also be improved by including triple corrections beyond the NO2B approximation. The crossing of the $Q_s(2_1^+)$ and $Q_s(2_2^+)$ values further demonstrates that the energy ordering of first two 2^+ states, built on the weakly deformed and strongly deformed configurations, respectively, is inverted going from ^{30}Mg to ^{32}Mg .

Figure 3 displays the low-lying states of ^{33}Mg , which exhibits shape-coexistence phenomena similar to ^{32}Mg , but with a significantly more complicated low-energy structure due to the additional coupling between the single-particle motion of the valence neutron with collective core excitations. This interplay is incorporated in our method, which explicitly accounts for all nucleons and the mixing of different configurations. The low-energy spectrum of ^{33}Mg is complicated by nearly-degenerate low-lying states, whose energy ordering is highly sensitive to the correlations embedded in the effective Hamiltonian. As shown in Fig. 3(c), when using the Hamiltonian $H(0)$, the spin-parity of the ground state of ^{33}Mg is pre-

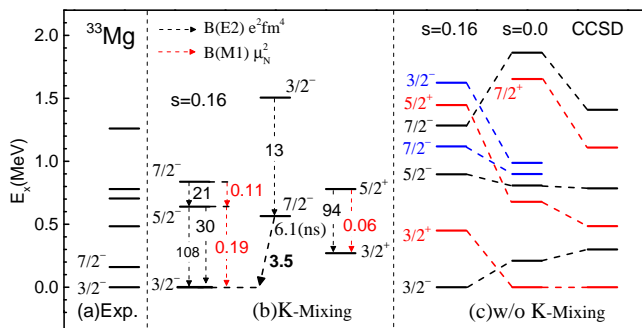


FIG. 3. Low-lying states of ^{33}Mg . Panel (a): Experimental data [19]. Panel (b): IM-GCM calculations with K -mixing for $s = 0.16 \text{ MeV}^{-1}$. Panel (c): IM-GCM calculations without K -mixing for $s = 0$ and 0.16 MeV^{-1} compared with projected CCSD results of Ref. [57].

TABLE I. The electric quadrupole moment (Q_s) and magnetic dipole moment (μ) of the $3/2_1^-$, $3/2_1^+$, and $7/2_1^-$ states in ^{33}Mg . Available experimental data are taken from Refs. [11, 80]

J^π	$Q_s(\text{efm}^2)$		$\mu(\mu_N)$	
	IM-GCM	Exp.	IM-GCM	Exp.
$3/2_1^-$	11.9	13.4(9.2)	-0.751	-0.7456(5)
$3/2_1^+$	9.7	-	1.078	-
$7/2_1^-$	-4.8	-	-0.783	-

dicted to be $3/2^+$, primarily driven by the $K^\pi = 3/2^+$ configuration in which the unpaired neutron occupies the $\Omega^\pi = 3/2^+$ component of the $\nu d_{3/2}$ orbital. This prediction is also found in the recent projected CCSD calculation [57], but it is not supported by the latest experimental data [19]. Similar to the case of ^{32}Mg , the single-particle shell structure is significantly altered as the flow parameter s increases. As a result, the $3/2_1^-$ state, dominated by the $K^\pi = 3/2^-$ configuration, becomes the ground state, while the $3/2_1^+$ state transitions to an excited state. We observe the same behavior for the ground state of ^{31}Mg , where the $1/2_1^+$ state becomes lower than the $3/2_1^+$ state once the IMSRG-evolved interaction is used [62]. This points again to the importance of dynamical correlations captured by the IMSRG flow. Moreover, we find that about two neutrons are promoted from the sd shell to the fp shell in ^{33}Mg , indicating that the $3/2_1^-$ state is primarily characterized by a $2p$ - $2h$ excitation across the $N = 20$ shell gap. Based on our predicted $E2$ transition strength and energy, we estimate the half-life of the $7/2_1^-$ state to be approximately 6.1 ns, which together with the distribution of the wave function [62] suggests this state to be a shape isomeric state. If the experimental energies are used, the half-life of the $7/2_1^-$ state is even longer, about $7.1 \mu\text{s}$. Notably, when K -mixing is neglected, the half-life significantly decreases to 76 ps, suggesting that K -mixing actually prolongs the half-life by reducing the transition energy. This offers a different perspective from that found in K -isomers, where K -mixing is known to accelerate decays [77–79].

The electric quadrupole moment Q_s and magnetic dipole moment μ of odd-mass nuclei are sensitive probes of the underlying nuclear shell structure and intrinsic configurations. For the low-lying states of ^{33}Mg , Table I shows that the magnitude of the Q_s for the $7/2_1^-$ state is notably smaller compared to the $3/2_1^-$ and $3/2_1^+$ states. This suggests that the $7/2_1^-$ state is dominated by weakly deformed configurations, while the $3/2_1^-$ and $3/2_1^+$ states are associated with strongly prolate-deformed configurations. This observation is consistent with the collective wave function distribution, as detailed in the supplementary material [62]. Additionally, the accurate reproduction of both Q_s and μ demonstrates the success of our method in capturing the low-energy structure of odd-mass nuclei, even with complex shapes. Finally, we applied our method to investigate the boundary of the island of inversion around $N = 20$. Our results reveal a diverse coexistence of weak, moderate, and strongly deformed shapes in the low-lying states of nuclei in this region, which we will explore in greater detail in future work.

Summary. In this article, we applied the IM-GCM method, using nuclear interactions derived from chiral effective field theory, to study neutron-rich nuclei near $N = 20$, where both weakly and strongly deformed low-lying states coexist. This includes the description of both even- and odd-mass nuclei. In this framework, dynamic correlations associated with particle-hole excitations are primarily captured through IMSRG evolution, while collective correlations related to pairing and deformation are included via the PGCM. Our results reveal that deformed ground states emerge naturally in the nuclei within the island of inversion through the IMSRG flow. The computed energy spectra and electromagnetic properties agree well with available experimental data, underscoring the importance of both dynamic and collective correlations for reproducing the ordering of states with distinct shapes. Notably, we predict the ground state of ^{33}Mg to have a spin-parity of $3/2^-$, while the lowest $7/2^-$ state likely corresponds to a shape isomer. The ground state is dominated by a strongly deformed configuration with $K^\pi = 3/2^-$, while the shape isomer arises from the mixing of weakly deformed configurations with different K values. This work provides new insights into the structure of neutron-rich nuclei, including odd-mass ones, and marks a significant step in applying *ab initio* methods to the problem of shape coexistence in medium-mass nuclei.

Acknowledgments. We thank D. Bazin, J. Engel, T. Papenbrock, Y. Sun, R. Wirth, and Y. N. Zhang for fruitful discussions, and thank Z. H. Sun for sending us the results of the angular-momentum projected coupled cluster calculation on ^{33}Mg for comparison. This work is supported in part by the National Natural Science Foundation of China (Grant Nos. 12375119, 12275369, and 12141501), the Guangdong Basic and Applied Basic Research Foundation (2023A1515010936). H.H. was funded by the U.S. Department of Energy, Office of Science, Office of Nuclear Physics DE-SC0023516 and DE-SC0023175 (SciDAC-5 NUCLEI Collaboration). T.R.R. acknowledges support from the Spanish MCIN under Contract PID2021-127890NB-I00. This

work was supported in part through computational resources and services provided by the Institute for Cyber-Enabled Research at Michigan State University, as well as the Beijing Super Cloud Computing Center (BSCC).

* yaojm8@sysu.edu.cn

† hergert@frib.msu.edu

- [1] K. Heyde and J. L. Wood, Shape coexistence in atomic nuclei, *Rev. Mod. Phys.* **83**, 1467 (2011).
- [2] W. Schwerdtfeger *et al.*, Shape Coexistence Near Neutron Number $N=20$: First Identification of the E-0 Decay from the Deformed First Excited $J^\pi=0^+$ State in Mg-30, *Phys. Rev. Lett.* **103**, 012501 (2009), arXiv:0808.0264 [nucl-ex].
- [3] F. Rotaru *et al.*, Unveiling the intruder deformed 0_2^+ state in ^{34}Si , *Phys. Rev. Lett.* **109**, 092503 (2012), arXiv:1206.6572 [nucl-ex].
- [4] P. Doornenbal, H. Scheit, S. Takeuchi, N. Aoi, K. Li, M. Matsushita, D. Steppenbeck, H. Wang, H. Baba, E. Ideguchi, N. Kobayashi, Y. Kondo, J. Lee, S. Michimasa, T. Motobayashi, A. Poves, H. Sakurai, M. Takechi, Y. Togano, and K. Yoneda, Mapping the deformation in the “island of inversion”: Inelastic scattering of ^{30}Ne and ^{36}Mg at intermediate energies, *Phys. Rev. C* **93**, 044306 (2016).
- [5] P. Doornenbal *et al.*, Exploring the ‘Island of Inversion’ by in-beam gamma-ray spectroscopy of the neutron-rich sodium isotopes $^{31,32,33}\text{Na}$, *Phys. Rev. C* **81**, 041305 (2010), arXiv:1003.2848 [nucl-ex].
- [6] K. Wimmer *et al.*, Discovery of the shape coexisting 0^+ state in ^{32}Mg by a two neutron transfer reaction, *Phys. Rev. Lett.* **105**, 252501 (2010), arXiv:1010.3999 [nucl-ex].
- [7] E. K. Warburton, J. A. Becker, and B. A. Brown, Mass systematics for $a=29-44$ nuclei: The deformed $a\sim 32$ region, *Phys. Rev. C* **41**, 1147 (1990).
- [8] E. Caurier, G. Martinez-Pinedo, F. Nowacki, A. Poves, and A. P. Zuker, The Shell Model as Unified View of Nuclear Structure, *Rev. Mod. Phys.* **77**, 427 (2005), arXiv:nucl-th/0402046.
- [9] E. Caurier, F. Nowacki, and A. Poves, Merging of the islands of inversion at $n = 20$ and $n = 28$, *Phys. Rev. C* **90**, 014302 (2014).
- [10] S. Nummela *et al.* (ISOLDE), Intruder features in the island of inversion: The case of Mg-33, *Phys. Rev. C* **64**, 054313 (2001).
- [11] D. T. Yordanov, M. Kowalska, K. Blaum, M. De Rydt, K. T. Flanagan, P. Lievens, R. Neugart, G. Neyens, and H. H. Stroke, Spin and Magnetic Moment of Mg-33: Evidence for a Negative-Parity Intruder Ground State, *Phys. Rev. Lett.* **99**, 212501 (2007).
- [12] V. Tripathi *et al.*, Intruder Configurations in the $A=33$ Isobars: Mg-33 and Al-33, *Phys. Rev. Lett.* **101**, 142504 (2008).
- [13] J. Li, Y. Zhang, J. M. Yao, and J. Meng, Magnetic moments of Mg-33 in time-odd relativistic mean field approach, *Sci. China G* **52**, 1586 (2009), arXiv:0910.4090 [nucl-th].
- [14] R. Kanungo *et al.*, Structure of Mg-33 sheds new light on the $N = 20$ island of inversion, *Phys. Lett. B* **685**, 253 (2010).
- [15] V. Tripathi *et al.*, Reply to ‘Comment on ‘Intruder Configurations in the $A=33$ Isobars: Mg-33 and Al-33’’, *Phys. Rev. Lett.* **104**, 129202 (2010).
- [16] D. T. Yordanov, K. Blaum, M. De Rydt, M. Kowalska, R. Neugart, G. Neyens, and I. Hamamoto, Comment on ‘Intruder Configurations in the $A=33$ Isobars: Mg-33 and Al-33’, *Phys. Rev. Lett.* **104**, 129201 (2010).
- [17] M. Kimura, Spectroscopy and intruder configurations of ^{33}Mg and ^{31}Ne studied with antisymmetrized molecular dynamics, (2011), arXiv:1105.3281 [nucl-th].
- [18] N. Kitamura *et al.*, Coexisting normal and intruder configurations in ^{32}Mg , *Phys. Lett. B* **822**, 136682 (2021), arXiv:2109.12090 [nucl-ex].
- [19] D. Bazin *et al.*, Spectroscopy of ^{33}Mg with knockout reactions, *Phys. Rev. C* **103**, 064318 (2021), arXiv:2101.12182 [nucl-ex].
- [20] R. R. Rodríguez-Guzmán, J. L. Egido, and L. M. Robledo, Description of quadrupole collectivity in $n \approx 20$ nuclei with techniques beyond the mean field, *Phys. Rev. C* **62**, 054319 (2000).
- [21] T. Nikšić, D. Vretenar, and P. Ring, Beyond the relativistic mean-field approximation: Configuration mixing of angular momentum projected wave functions, *Phys. Rev. C* **73**, 034308 (2006), arXiv:nucl-th/0601005.
- [22] J. M. Yao, H. Mei, H. Chen, J. Meng, P. Ring, and D. Vretenar, Configuration mixing of angular-momentum projected triaxial relativistic mean-field wave functions. II. Microscopic analysis of low-lying states in magnesium isotopes, *Phys. Rev. C* **83**, 014308 (2011), arXiv:1006.1400 [nucl-th].
- [23] D. Lee, Lattice simulations for few- and many-body systems, *Prog. Part. Nucl. Phys.* **63**, 117 (2009), arXiv:0804.3501 [nucl-th].
- [24] P. Navrátil, S. Quaglioni, I. Stetcu, and B. R. Barrett, Recent developments in no-core shell-model calculations, *J. Phys. G* **36**, 083101 (2009), arXiv:0904.0463 [nucl-th].
- [25] B. R. Barrett, P. Navrátil, and J. P. Vary, Ab initio no core shell model, *Prog. Part. Nucl. Phys.* **69**, 131 (2013).
- [26] V. Somà, A. Cipollone, C. Barbieri, P. Navrátil, and T. Duguet, Chiral two- and three-nucleon forces along medium-mass isotope chains, *Phys. Rev. C* **89**, 061301 (2014), arXiv:1312.2068 [nucl-th].
- [27] G. Hagen, T. Papenbrock, M. Hjorth-Jensen, and D. J. Dean, Coupled-cluster computations of atomic nuclei, *Rept. Prog. Phys.* **77**, 096302 (2014), arXiv:1312.7872 [nucl-th].
- [28] J. Carlson, S. Gandolfi, F. Pederiva, S. C. Pieper, R. Schiavilla, K. E. Schmidt, and R. B. Wiringa, Quantum Monte Carlo methods for nuclear physics, *Rev. Mod. Phys.* **87**, 1067 (2015), arXiv:1412.3081 [nucl-th].
- [29] K. D. Launey, T. Dytrych, and J. P. Draayer, Symmetry-guided large-scale shell-model theory, *Prog. Part. Nucl. Phys.* **89**, 101 (2016), arXiv:1612.04298 [nucl-th].
- [30] H. Hergert, S. K. Bogner, T. D. Morris, A. Schwenk, and K. Tsukiyama, The In-Medium Similarity Renormalization Group: A Novel Ab Initio Method for Nuclei, *Phys. Rept.* **621**, 165 (2016), arXiv:1512.06956 [nucl-th].
- [31] S. Weinberg, Effective chiral Lagrangians for nucleon - pion interactions and nuclear forces, *Nucl. Phys. B* **363**, 3 (1991).
- [32] E. Epelbaum, H.-W. Hammer, and U.-G. Meißner, Modern theory of nuclear forces, *Rev. Mod. Phys.* **81**, 1773 (2009).
- [33] R. Machleidt and D. R. Entem, Chiral effective field theory and nuclear forces, *Phys. Rept.* **503**, 1 (2011), arXiv:1105.2919 [nucl-th].
- [34] T. Dytrych, K. D. Launey, J. P. Draayer, D. Rowe, J. Wood, G. Rosensteel, C. Bahri, D. Langr, and R. B. Baker, Physics of nuclei: Key role of an emergent symmetry, *Phys. Rev. Lett.* **124**, 042501 (2020), arXiv:1810.05757 [nucl-th].
- [35] A. E. McCoy, M. A. Caprio, P. Maris, and P. J. Fasano, Intruder band mixing in an ab initio description of ^{12}Be , *Phys. Lett. B* **856**, 138870 (2024), arXiv:2402.12606 [nucl-th].
- [36] K. Tsukiyama, S. K. Bogner, and A. Schwenk, In-Medium Similarity Renormalization Group for Nuclei, *Phys. Rev. Lett.* **106**, 222502 (2011), arXiv:1006.3639 [nucl-th].
- [37] K. Tsukiyama, S. K. Bogner, and A. Schwenk, In-Medium

- Similarity Renormalization Group for Open-Shell Nuclei, Phys. Rev. C **85**, 061304 (2012), arXiv:1203.2515 [nucl-th].
- [38] S. R. Stroberg, A. Calci, H. Hergert, J. D. Holt, S. K. Bogner, R. Roth, and A. Schwenk, Nucleus-dependent valence-space approach to nuclear structure, Phys. Rev. Lett. **118**, 032502 (2017).
- [39] S. R. Stroberg, S. K. Bogner, H. Hergert, and J. D. Holt, Nonempirical Interactions for the Nuclear Shell Model: An Update, Ann. Rev. Nucl. Part. Sci. **69**, 307 (2019), arXiv:1902.06154 [nucl-th].
- [40] S. R. Stroberg, J. D. Holt, A. Schwenk, and J. Simonis, *AbInitio* Limits of Atomic Nuclei, Phys. Rev. Lett. **126**, 022501 (2021), arXiv:1905.10475 [nucl-th].
- [41] B. Hu *et al.*, Ab initio predictions link the neutron skin of ^{208}Pb to nuclear forces, Nature Phys. **18**, 1196 (2022), arXiv:2112.01125 [nucl-th].
- [42] T. Miyagi, X. Cao, R. Seutin, S. Bacca, R. F. Garcia Ruiz, K. Hebeler, J. D. Holt, and A. Schwenk, Impact of Two-Body Currents on Magnetic Dipole Moments of Nuclei, Phys. Rev. Lett. **132**, 232503 (2024), arXiv:2311.14383 [nucl-th].
- [43] N. M. Parzuchowski, S. R. Stroberg, P. Navrátil, H. Hergert, and S. K. Bogner, Ab initio electromagnetic observables with the in-medium similarity renormalization group, Phys. Rev. C **96**, 034324 (2017).
- [44] J. Henderson, G. Hackman, P. Ruotsalainen, S. Stroberg, K. Launey, J. Holt, F. Ali, N. Bernier, M. Bentley, M. Bowry, R. Caballero-Folch, L. Evitts, R. Frederick, A. Garnsworthy, P. Garrett, B. Jigmeddorj, A. Kilic, J. Lassen, J. Measures, D. Muecher, B. Olaizola, E. O’Sullivan, O. Paetkau, J. Park, J. Smallcombe, C. Svensson, R. Wadsworth, and C. Wu, Testing microscopically derived descriptions of nuclear collectivity: Coulomb excitation of ^{22}Mg , Phys. Lett. B **782**, 468 (2018).
- [45] T. Miyagi, S. R. Stroberg, J. D. Holt, and N. Shimizu, Ab initio multishell valence-space Hamiltonians and the island of inversion, Phys. Rev. C **102**, 034320 (2020), arXiv:2004.12969 [nucl-th].
- [46] S. R. Stroberg, J. Henderson, G. Hackman, P. Ruotsalainen, G. Hagen, and J. D. Holt, Systematics of $e2$ strength in the sd shell with the valence-space in-medium similarity renormalization group, Phys. Rev. C **105**, 034333 (2022).
- [47] H. Hergert, S. Binder, A. Calci, J. Langhammer, and R. Roth, Ab Initio Calculations of Even Oxygen Isotopes with Chiral Two-Plus-Three-Nucleon Interactions, Phys. Rev. Lett. **110**, 242501 (2013), arXiv:1302.7294 [nucl-th].
- [48] E. Gebrerufael, K. Vobig, H. Hergert, and R. Roth, Ab Initio Description of Open-Shell Nuclei: Merging No-Core Shell Model and In-Medium Similarity Renormalization Group, Phys. Rev. Lett. **118**, 152503 (2017), arXiv:1610.05254 [nucl-th].
- [49] J. M. Yao, J. Engel, L. J. Wang, C. F. Jiao, and H. Hergert, Generator-coordinate reference states for spectra and $0\nu\beta\beta$ decay in the in-medium similarity renormalization group, Phys. Rev. C **98**, 054311 (2018), arXiv:1807.11053 [nucl-th].
- [50] J. M. Yao, B. Bally, J. Engel, R. Wirth, T. R. Rodríguez, and H. Hergert, Ab initio treatment of collective correlations and the neutrinoless double beta decay of ^{48}Ca , Phys. Rev. Lett. **124**, 232501 (2020).
- [51] M. Frosini, T. Duguet, J.-P. Ebran, and V. Somà, Multi-reference many-body perturbation theory for nuclei: I. Novel PGCM-PT formalism, Eur. Phys. J. A **58**, 62 (2022), arXiv:2110.15737 [nucl-th].
- [52] M. Frosini, T. Duguet, J.-P. Ebran, B. Bally, T. Mongelli, T. R. Rodríguez, R. Roth, and V. Somà, Multi-reference many-body perturbation theory for nuclei: II. Ab initio study of neon isotopes via PGCM and IM-NCSM calculations, Eur. Phys. J. A **58**, 63 (2022), arXiv:2111.00797 [nucl-th].
- [53] M. Frosini, T. Duguet, J.-P. Ebran, B. Bally, H. Hergert, T. R. Rodríguez, R. Roth, J. Yao, and V. Somà, Multi-reference many-body perturbation theory for nuclei: III. Ab initio calculations at second order in PGCM-PT, Eur. Phys. J. A **58**, 64 (2022), arXiv:2111.01461 [nucl-th].
- [54] G. Hagen, S. J. Novario, Z. H. Sun, T. Papenbrock, G. R. Jansen, J. G. Lietz, T. Duguet, and A. Tichai, Angular-momentum projection in coupled-cluster theory: Structure of Mg^{34} , Phys. Rev. C **105**, 064311 (2022), arXiv:2201.07298 [nucl-th].
- [55] Z. H. Sun, A. Ekström, C. Forssén, G. Hagen, G. R. Jansen, and T. Papenbrock, Multiscale physics of atomic nuclei from first principles (2024) arXiv:2404.00058 [nucl-th].
- [56] B. S. Hu, Z. H. Sun, G. Hagen, and T. Papenbrock, Ab initio computations of strongly deformed nuclei near Zr^{80} , Phys. Rev. C **110**, L011302 (2024), arXiv:2405.05052 [nucl-th].
- [57] Z. H. Sun, T. R. Djärv, G. Hagen, G. R. Jansen, and T. Papenbrock, Structure of odd-mass Ne, Na, and Mg nuclei, (2024), arXiv:2409.02279 [nucl-th].
- [58] J. M. Yao, M. Bender, and P.-H. Heenen, Systematics of low-lying states of even-even nuclei in the neutron-deficient lead region from a beyond-mean-field calculation, Phys. Rev. C **87**, 034322 (2013).
- [59] D. R. Entem and R. Machleidt, Accurate charge-dependent nucleon-nucleon potential at fourth order of chiral perturbation theory, Phys. Rev. C **68**, 041001 (2003).
- [60] S. K. Bogner, R. J. Furnstahl, and A. Schwenk, From low-momentum interactions to nuclear structure, Prog. Part. Nucl. Phys. **65**, 94 (2010), arXiv:0912.3688 [nucl-th].
- [61] K. Hebeler, S. K. Bogner, R. J. Furnstahl, A. Nogga, and A. Schwenk, Improved nuclear matter calculations from chiral low-momentum interactions, Phys. Rev. C **83**, 031301 (2011).
- [62] See supplemental material [url] for a detailed introduction to the *imsrg*-evolved tensor operators and other applications, .
- [63] T. D. Morris, N. Parzuchowski, and S. K. Bogner, Magnus expansion and in-medium similarity renormalization group, Phys. Rev. C **92**, 034331 (2015), arXiv:1507.06725 [nucl-th].
- [64] H. Hergert, In-Medium Similarity Renormalization Group for Closed and Open-Shell Nuclei, Phys. Scripta **92**, 023002 (2017), arXiv:1607.06882 [nucl-th].
- [65] W. Lin, E. F. Zhou, J. Yao, and H. Hergert, Quantum-Number Projected Generator Coordinate Method for ^{21}Ne with a Chiral Two-Nucleon-Plus-Three-Nucleon Interaction, Symmetry **16**, 409 (2024), arXiv:2403.01177 [nucl-th].
- [66] P. Ring and P. Schuck, *The nuclear many-body problem* (Springer-Verlag, New York, 1980).
- [67] B. Bally and M. Bender, Projection on particle number and angular momentum: Example of triaxial bogoliubov quasiparticle states, Phys. Rev. C **103**, 024315 (2021).
- [68] D. L. Hill and J. A. Wheeler, Nuclear constitution and the interpretation of fission phenomena, Phys. Rev. **89**, 1102 (1953).
- [69] T. Duguet, H. Hergert, J. D. Holt, and V. Somà, Nonobservable nature of the nuclear shell structure: Meaning, illustrations, and consequences, Phys. Rev. C **92**, 034313 (2015).
- [70] C. R. Ding, C. C. Wang, J. M. Yao, H. Hergert, *et al.*, in preparation (2024).
- [71] J. M. Yao, Symmetry Restoration Methods, in *Handbook of Nuclear Physics*, edited by I. Tanihata, H. Toki, and T. Kajino (2022) pp. 1–36, arXiv:2204.12126 [nucl-th].
- [72] National Nuclear Data Center, NuDat 2 Database (2020), <https://www.nndc.bnl.gov/nudat2>.
- [73] T. Otsuka, A. Gade, O. Sorlin, T. Suzuki, and Y. Utsuno, Evo-

- lution of shell structure in exotic nuclei, *Rev. Mod. Phys.* **92**, 015002 (2020).
- [74] A. Bellei, J. M. Yao, B. Bally, J. Pitcher, J. Engel, H. Hergert, J. D. Holt, T. Miyagi, T. R. Rodríguez, A. M. Romero, S. R. Stroberg, and X. Zhang, Ab initio uncertainty quantification of neutrinoless double-beta decay in ^{76}Ge , *Phys. Rev. Lett.* **132**, 182502 (2024).
- [75] S. R. Stroberg, T. D. Morris, and B. C. He, In-medium similarity renormalization group with flowing 3-body operators, and approximations thereof, *Phys. Rev. C* **110**, 044316 (2024).
- [76] B. C. He and S. R. Stroberg, Factorized approximation to the in-medium similarity renormalization group *imsrg(3)*, *Phys. Rev. C* **110**, 044317 (2024).
- [77] K. E. G. Löbner, Systematics of absolute transition probabilities of K-Forbidden gamma-ray transitions, *Phys. Lett. B* **26**, 369 (1968).
- [78] P. Walker and G. Dracoulis, Energy traps in atomic nuclei, *Nature* **399**, 35 (1999).
- [79] F.-Q. Chen, Y. Sun, P. M. Walker, G. D. Dracoulis, Y. R. Shimizu, and J. A. Sheikh, Mixing effects on K-forbidden transition rates from the 6+ isomers in the N = 104 isotones, *J. Phys. G* **40**, 015101 (2013).
- [80] D. T. Yordanov *et al.*, Quadrupole moments of ^{29}Mg and ^{33}Mg , *Hyperfine Interact.* **240**, 67 (2019), arXiv:1905.05580 [nucl-ex].